

## Nanoindentation Study of Polydimethylsiloxane Elastic Modulus Using Berkovich and Flat Punch Tips

Zhixin Wang, Alex A. Volinsky, Nathan D. Gallant

Department of Mechanical Engineering, University of South Florida, Tampa, Florida 33620

Correspondence to: A. A. Volinsky (E-mail: volinsky@usf.edu)

**ABSTRACT:** This article explores polydimethylsiloxane (PDMS) mechanical properties, and presents nanoindentation experiments with Berkovich and flat punch indenters. In the Berkovich tip quasi-static nanoindentation test, there are pull-in and pull-off events observed during the initial tip contact, and when withdrawing from the surface, respectively. The pull-in interaction needs to be accounted for to properly determine the initial contact point, and thus the accurate contact area. Once accounted for the pull-in event, the Berkovich and flat punch tips quasi-static nanoindentation tests give comparable results of about 1.5 MPa for the PDMS elastic modulus (5 : 1 elastomer base to the curing agent ratio). However, PDMS unloading stiffness is higher than the loading stiffness, and dynamic PDMS testing yields higher elastic modulus of about 3.6 MPa. While these results are comparable with the large strain macroscopic compression test results, the difference underscores the complexity of elastomer mechanical characterization and illustrates the discrepancies typical of the reported values. This article describes nanoindentation methods and critical aspects of interpreting results to assess PDMS mechanical properties. © 2014 Wiley Periodicals, Inc. *J. Appl. Polym. Sci.* **2015**, *132*, 41384.

**KEYWORDS:** crosslinking; mechanical properties; properties and characterization; viscosity and viscoelasticity

Received 17 June 2014; accepted 8 August 2014

DOI: 10.1002/app.41384

### INTRODUCTION

Polydimethylsiloxane (PDMS) is one of the most widely used silicon-based organic polymers.<sup>1</sup> PDMS has been utilized as the substrate to grow cells, because of its controllable wide range of elastic properties,<sup>2–5</sup> since local stiffness of the substrate affects cells behavior. To characterize PDMS mechanical properties, various approaches, including nanoindentation techniques can be used.<sup>6</sup> The previous study utilized a custom-built macroscopic compression instrument for measuring macroscopic elastic properties of PDMS samples with the 5 : 1 to 33 : 1 elastomer base to the curing agent ratios.<sup>7</sup> However, nanoindentation is capable of providing better surface sensitivity and spatial resolution.

Testing elastomer mechanical properties using nanoindentation is still quite novel and challenging, thus there are not many references available in the literature. Some PDMS samples, especially those with low curing agent concentrations are relatively soft, with the elastic modulus well below 1 MPa.<sup>7</sup> As a result, the maximum load is quite small, even at the maximum displacement range of the nanoindenter, which is typically on the order of a few microns. Additionally, most PDMS samples are tacky, making it quite challenging to determine the initial point of contact of the indenter tip, based on which the contact area and the elastic modulus are calculated. Advanced *in situ* tests inside the scanning electron microscope<sup>8</sup> or dynamic nanoindentation testing approaches<sup>9</sup> have

been utilized to accurately determine the contact area or the initial contact point during indentation. Utilizing a flat punch tip geometry, for which the contact area stays constant, is one of the alternatives. Conventional dynamic mechanical analysis (DMA) testing can be a viable method to test the complex PDMS modulus.<sup>10</sup> In addition to the quasi-static indentation, dynamic nanoindentation testing was also employed here. In this article, various nanoindentation-based methods using different tip geometries have been utilized to characterize mechanical properties of the 5 : 1 PDMS sample. The base/agent mass ratio determines the PDMS elastic properties.<sup>11</sup> In the previous study, which utilized the custom-built macroscopic compression tester, the 5 : 1 PDMS sample elastic modulus was measured at  $3.59 \pm 0.11$  MPa.<sup>7</sup> The elastic modulus,  $E$ , in MPa can be expressed as a function of the PDMS base/curing agent weight ratio,  $n$ , as:<sup>7</sup>

$$E = \frac{20\text{MPa}}{n} \quad (1)$$

For the same base/curing agent ratio, PDMS elastic modulus measured in compression<sup>12</sup> seems to be higher than in tension.<sup>13</sup>

### MATERIALS AND METHODS

#### Sample Preparation

Sylgard 184 silicone elastomer base and silicone elastomer curing agent with the 5 : 1 base/agent mass ratio, manufactured by

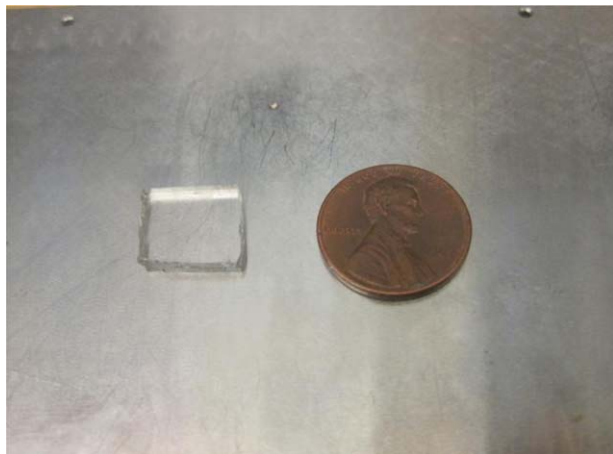


**Figure 1.** PDMS sample mounted on the Hysitron Triboindenter stage. [Color figure can be viewed in the online issue, which is available at [wileyonlinelibrary.com](http://wileyonlinelibrary.com).]

the Dow Corning (Midland, MI) were used to make the PDMS samples.<sup>14</sup> Sheets of PDMS (3 mm thick) were produced by thoroughly mixing the elastomer base and the curing agent, then pouring the mixture into a flat bottom polystyrene dish and degassing it under vacuum to remove air bubbles. Then the 5 : 1 PDMS was cured in an oven for 1 h at 65°C.

#### Sample Mounting

To accommodate the nanoindentation workspace, the prepared PDMS sheets were cut into 1 cm<sup>2</sup> square pads with a utility knife. Instead of the typical glue mounting of the sample, it was placed directly onto the Hysitron Triboindenter stage and pressed with tweezers to develop full contact with the stage, evident by the air escaping along the interface between the sample and the steel sample stage holder (Figure 1).

#### Nanoindentation Testing

The Hysitron Triboindenter (Hysitron, USA) was used for all three types of nanoindentation tests. The 5 : 1 PDMS sample was tested using quasi-static nanoindentation with the Berkovich and flat punch tips. It was also tested dynamically with the flat punch tip, which had cylindrical shape and a diameter of 1002.19 μm. Relaxation tests with different unloading rates were conducted to assess PDMS viscoelastic properties. Nanoindentation dynamic mechanical analysis (nano-DMA) was also conducted to quantify PDMS storage and loss elastic modulus.

The nanoindenter transducer with the corresponding mounted indenter tip was calibrated before each experiment. Initially an automated quick approach was utilized to make the contact with the sample surface. However, automated features of the instrument to make the indents with the Berkovich tip were not utilized. The tip was manually positioned 1–2 μm above the sample surface, making sure that there was no contact with the sample prior to each indent. This way the whole interaction between the Berkovich tip and the PDMS sample was captured, including the pull-in and the pull-off events. Each nanoindentation test was conducted once at a new location on the sample to avoid the Mullins effect.<sup>15,16</sup>

For the quasi-static nanoindentation test, the reduced modulus of the sample is calculated as:

$$E_r = \frac{S\sqrt{\pi}}{2\sqrt{A}} \quad (2)$$

where  $S$  is the slope of the upper portion of the unloading curve and  $A$  is the tip contact area, which for the perfect Berkovich tip is related to the indentation depth,  $h$ , as:

$$A = 24.5h^2 \quad (3)$$

The tip area function was also obtained by making indents into the fused quartz standard sample with the reduced modulus of 69.6 GPa. Measured reduced modulus,  $E_r$ , is related to the PDMS elastic modulus,  $E_{\text{PDMS}}$ , as:

$$\frac{1}{E_r} = \frac{(1 - \nu_{\text{PDMS}}^2)}{E_{\text{PDMS}}} + \frac{(1 - \nu_{\text{tip}}^2)}{E_{\text{tip}}} \quad (4)$$

Here,  $\nu_{\text{PDMS}}$  is the PDMS Poisson's ratio (0.5),<sup>17,18</sup> and  $\nu_{\text{tip}}$  is the Poisson's ratio of the diamond indenter (0.07). Since the elastic modulus of the diamond indenter tip (1140 GPa) is orders of magnitude larger than the PDMS elastic modulus (MPa), the second term in eq. (4) is negligible. The PDMS elastic modulus is related to the reduced modulus as:

$$E_{\text{PDMS}} = E_r(1 - \nu_{\text{PDMS}}^2) = 0.75E_r \quad (5)$$

Most nanoindentation studies report reduced modulus for PDMS, thus it is important to realize that the actual PDMS modulus is 25% lower than the reduced modulus, especially when making comparisons with other testing methods, including macroscopic compression or tensile tests.

In theory, for the flat punch tip, the contact area does not change with the indentation depth. However, it is important to make sure that the tip and the sample are in full contact, which requires a certain amount of pre-loading. Incomplete contact between the flat punch indenter tip and the sample surface occurs because of the misalignment tilt. Therefore, a pre-loading method was used to perform the flat punch nanoindentation tests. The flat punch with 1002.19 μm diameter and the sample surface were not parallel due to a slight misalignment tilt. Thus, to achieve full contact between the flat punch and the sample, the stage was moved upward in 5 μm increments, for the 40 μm total displacement. After 40 μm total displacement into the sample, the load started to change linearly with displacement, meaning that the tip and the sample had developed full contact. When the transducer is not actuated during pre-loading, its center plate will move due to the sample pushing on the tip. The stiffness of the sample is around 20 times of the stiffness of the transducer spring. Based on the 167 N/m spring constant of the transducer, the flat punch was displaced into the sample surface by over a micron, taking care of the initial tilt. During this procedure, one has to be careful not to break the transducer, as the distance between the plates of the transducer is about 80 μm. Once the full contact between the flat punch and the sample surface was established, the contact area remains constant during the test, thus eq. (2) can be rewritten for the cylindrical flat punch with the diameter  $D$ , as:

$$E_r = \frac{S}{D} \quad (6)$$

From the unloading slope,  $S$ , the reduced modulus of the sample can be obtained.

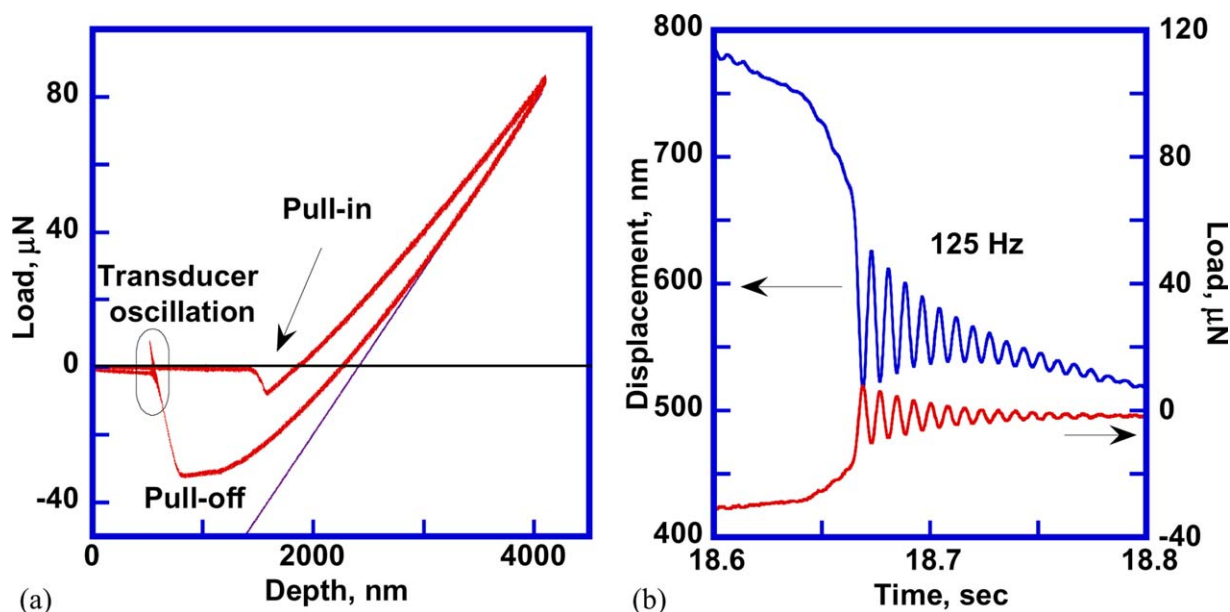


**Figure 2.** Berkovich tip nanoindentation of the 5 : 1 PDMS: (a) Load–displacement curve showing the pull-in and the pull-off phenomena; (b) transducer oscillation upon complete withdrawal from the sample. [Color figure can be viewed in the online issue, which is available at [wileyonlinelibrary.com](http://wileyonlinelibrary.com).]

The Hysitron Triboindenter is also capable of dynamic testing, which was used in this study as well for measuring storage and loss modulus. There are three test variables that can be controlled for the nano-DMA test: frequency, dynamic, and static forces. For the time-dependent behavior, dynamic testing offers the advantage of significantly decreased testing time by examining mechanical properties over a range of frequencies.<sup>19–21</sup> The storage,  $E'$ , and loss,  $E''$ , modulus in the DMA method are calculated as:

$$E' = \frac{k_s \sqrt{\pi}}{2\sqrt{A}} \quad (7)$$

$$E'' = \frac{\omega C_s \sqrt{\pi}}{2\sqrt{A}} \quad (8)$$

where  $k_s$  is the measured storage stiffness of the sample,  $C_s$  is the measured loss stiffness of the sample,  $\omega$  is the loading frequency, and  $A$  is the contact area, which does not change with the indentation depth for the flat punch tip. Thus, eqs. (7) and (8) for the flat punch indenter tip with the diameter  $D$  reduced to:

$$E' = \frac{k_s}{D} \quad (9)$$

$$E'' = \frac{\omega C_s}{D} \quad (10)$$

Based on the storage and loss modulus, the reduced modulus is:

$$E_r = \sqrt{E'^2 + E''^2} = \frac{\sqrt{k_s^2 + \omega^2 C_s^2}}{D} \quad (11)$$

## RESULTS AND DISCUSSION

### Berkovich Tip Nanoindentation

Figure 2(a) shows a typical load–displacement curve obtained by indenting 5 : 1 PDMS with the Berkovich tip. For the maxi-

mum transducer travel range of about 5  $\mu\text{m}$ , the maximum load is only just above 80  $\mu\text{N}$ . For softer PDMS samples the corresponding load is even smaller. The sample surface is quite tacky, thus the tip is attracted to it, resulting in the negative load measured by the transducer at the beginning of the indentation process, the so-called pull-in force. As a result, the initial contact point, used for calculating the contact area and the reduced modulus in the nanoindenter software, is shifted. Thus, the reduced modulus values automatically calculated by the software are not quite accurate. Some earlier nanoindentation studies utilized an automated surface approach and ignored this initial contact adhesion force effect, reporting only the positive load portion of the load–displacement curve in Figure 2(a).<sup>6,22</sup> The problem of accurately determining the indentation contact area of PDMS has been solved as described in a report of *in situ* indentation in the scanning electron microscope.<sup>8</sup> Alternatively, the adhesion force effect can be eliminated by making indents with spherical tips in contact lens solution.<sup>23</sup> After the pull-in phenomenon, the nanoindentation load starts to increase as the tip pushes against the sample surface. For this composition, the pull-in interaction happened over an  $\sim 400$  nm displacement range, while the pull-off interaction was over a micron. When the initial tip–sample interaction was properly accounted for by shifting the initial contact point of the load–displacement curve to the minimum of the pull-in event, the 5 : 1 PDMS reduced elastic modulus measured using the Berkovich tip nanoindentation was  $2 \pm 0.07$  MPa, an average of three tests, which corresponds to an elastic modulus of about 1.5 MPa. The pull-off phenomenon has been used to measure PDMS elastic properties using a large radius spherical tip indenter.<sup>24</sup>

At the end of the indentation process, the tip was withdrawn from the sample's surface. As the tip detached from the sample

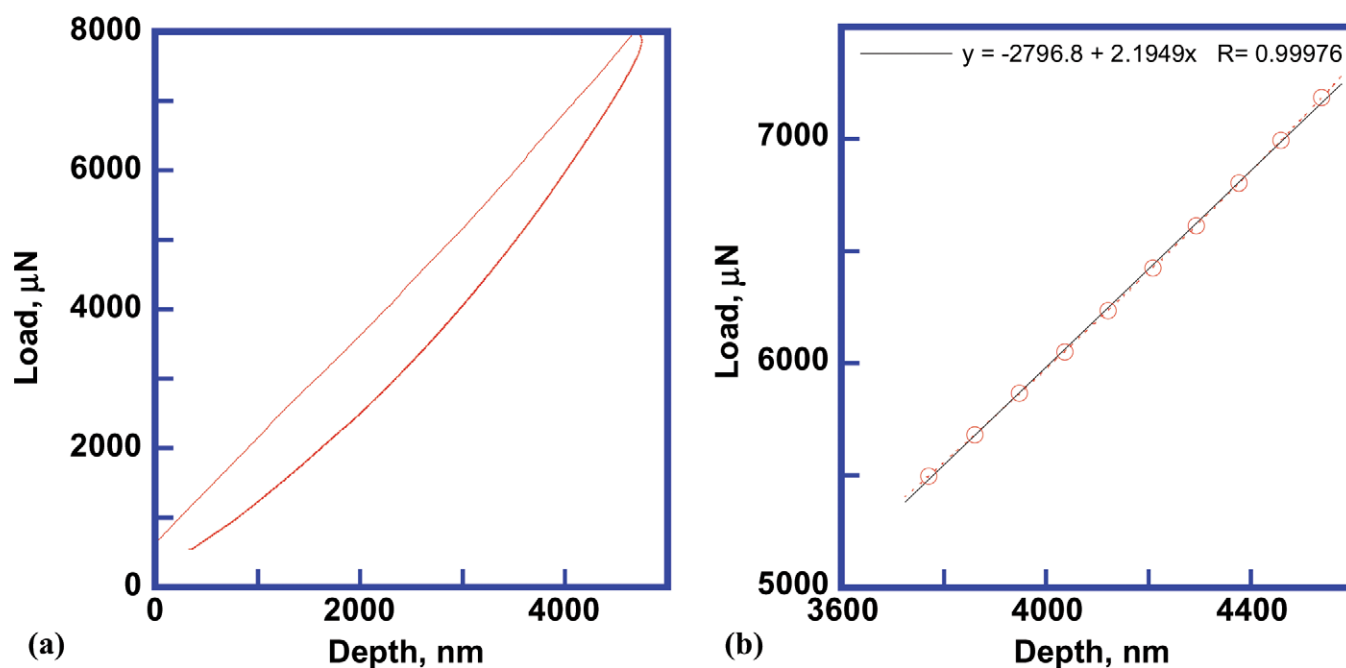


**Figure 3.** Flat punch nanoindentation of the 5 : 1 PDMS: (a) Load–displacement curve; (b) linear fit of the upper unloading portion of the nanoindentation curve in (a). [Color figure can be viewed in the online issue, which is available at [wileyonlinelibrary.com](http://wileyonlinelibrary.com).]

surface, the pull-off event was followed by damped oscillation of the transducer. Figure 2(b) plots nanoindentation load and depth over time, where the effect is clearly seen in more detail. The oscillation frequency is 125 Hz, which is close to the measured transducer resonance frequency of 126 Hz.

#### Quasi-Static Flat Punch Nanoindentation

The initial tip interaction effects associated with the Berkovich tip indentation can also be avoided by using a flat punch tip.<sup>25,26</sup> As long as the tip develops full contact with the surface, eq. (6) can be used to calculate the elastic modulus. A typical flat punch nanoindentation load–displacement curve is shown in Figure 3(a). A linear fit to the upper portion of the unloading curve is shown in Figure 3(b). Based on eq. (6), the reduced elastic modulus of the 5 : 1 PDMS sample is  $2.12 \pm 0.04$  MPa (average of three tests), which is close to the Berkovich tip indentation result of  $2 \pm 0.07$  MPa, and corresponds to about 1.6 MPa elastic modulus.

Similar experiments were performed using different unloading rates, as seen in Figure 4(a). The sample was rapidly loaded to the maximum load of 8 mN in 2 sec, followed by unloading over 60 sec to 400 sec. PDMS clearly exhibits viscoelastic behavior, followed by recovery during the nanoindentation unloading. This recovery behavior depends on the unloading rate.<sup>27</sup> Here, fast 2 sec loading was used, followed by the unloading at different rates. If the tip was unloaded at the same fast rate as the loading, it would simply lose contact with the sample. Figure 4(b) shows the quantitative relationship between the PDMS nanoindentation recovery in terms of the maximum displacement recovery in % and the unloading rate.<sup>28</sup> The sample deformation recovers almost completely if long enough time is allowed for relaxation, signifying the viscoelastic nature of the deformation.

It should be noted that the initial unloading slope is higher than the loading slope in Figures 3(a) and 4(a). During indentation of elastic–plastic materials the steeper unloading slope is due to the plastic deformation that occurs during loading, i.e. the loading slope is less steep due to the sample plastic deformation. In this case there is almost complete deformation recovery upon the unloading, especially for the longer unloading times. Similar effects in PDMS have been observed using conospherical indenter geometry.<sup>6</sup> The unloading stiffness appears higher than the loading stiffness due to the viscoelastic nature of the slow unloading process, resulting in elevated values of the elastic modulus calculated from the unloading data.

#### Dynamic Flat Punch Nanoindentation

Dynamic testing using nano-DMA was performed to obtain loss and storage modulus of the PDMS sample. First, the dynamic transducer response with the attached flat punch tip was acquired for proper calibration (Figure 5). Based on the data in Figure 5, the tip with the transducer center plate mass was determined at 260.23 mg, the center plate spring constant,  $k_i$  was 166.73 N/m, damping,  $C_i$  was 0.0141 kg/sec, and the transducer resonance frequency was 126 Hz. These values were used for properly measuring the sample storage and loss stiffnesses, automatically calculated by the nanoindenter software, based on the dynamic model,<sup>29</sup> accounting for the dynamic transducer response. The resonant frequency of 126 Hz, measured with the flat punch tip, is close to the 125 Hz frequency of the transducer oscillation with the Berkovich tip. The slight frequency difference is due to the different mass of the two indenter tips.

Similar to the quasi-static flat punch indentation, the pre-loading method was used to develop full contact between the flat punch and the PDMS sample prior to indentation. Using the measured sample storage and loss stiffnesses, it was possible



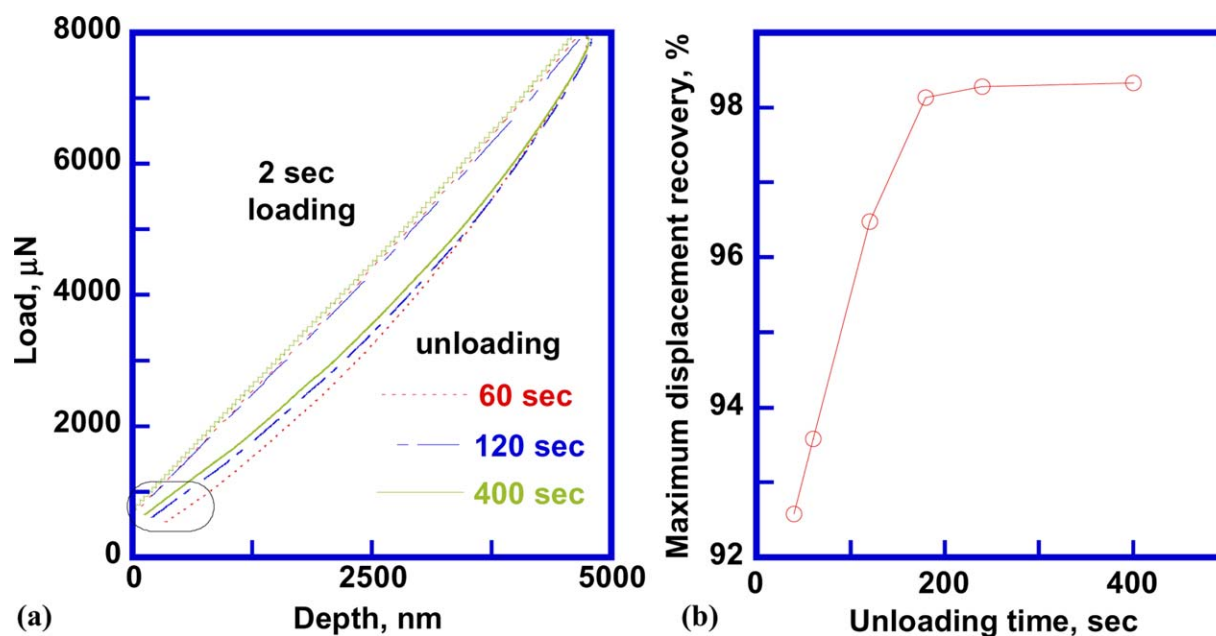


**Figure 4.** PDMS nanoindentation: (a) recovery behavior with different unloading time; (b) displacement recovery dependence on the unloading time. [Color figure can be viewed in the online issue, which is available at [wileyonlinelibrary.com](http://wileyonlinelibrary.com).]

to calculate the storage and the loss modulus using eqs. (7) and (8), respectively. Figure 6(a) shows the storage modulus of the 5 : 1 PDMS sample, obtained from the frequency control tests. The tip oscillation frequency was varied from either 2.5 Hz, or 10 Hz to 300 Hz. For the first test 1 mN static force was used, corresponding to 380 nm displacement into the sample with 50  $\mu\text{N}$  dynamic force oscillation. For the second test, 2 mN static force was used, corresponding to 1140 nm displacement into the sample with 100  $\mu\text{N}$  dynamic force oscillation. PDMS storage modulus increases with the test frequency, reaching the maximum above 200 Hz. At the low frequency, the nano-DMA

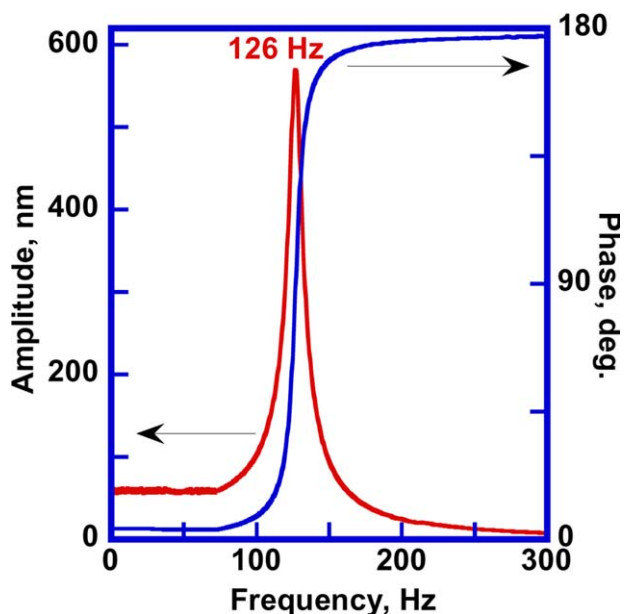


**Figure 5.** Transducer dynamic calibration. [Color figure can be viewed in the online issue, which is available at [wileyonlinelibrary.com](http://wileyonlinelibrary.com).]

results are similar to the flat punch quasi-static tests. In Figure 6(a), it is easy to see that the 5 : 1 PDMS storage modulus is around 3.5 MPa when the frequency is 10 Hz at the nanoindentation depth of 380 nm, which is comparable to the macroscopic compression test result.<sup>7</sup> The storage modulus is around 4.4 MPa when the frequency is 100 Hz with the nanoindentation depth at 1140 nm. For the frequency controlled test, the storage modulus strongly depends on the indentation depth, determined by the used static and dynamic forces. Larger indentation depth and higher loading frequency correspond to higher dynamic stiffness. Data points at 10 Hz and 100 Hz are outlined for comparison with the further displacement controlled tests conducted at these two fixed frequencies.

Figure 6(b) shows the 5 : 1 PDMS loss modulus obtained by the nano-DMA frequency control test. Similar to the storage modulus, the loss modulus strongly depended on the indentation depth at which the test was conducted, along with the dynamic force amplitude. For the 1 mN static and 50  $\mu\text{N}$  dynamic forces, the loss modulus reached the maximum at around 65 Hz. For the 2 mN static and 100  $\mu\text{N}$  dynamic forces, the loss modulus reaches the maximum at around 100 Hz, closer to the transducer resonance frequency. Using eqs. (5) and (11), the maximum elastic modulus of 3.55 MPa was calculated, reaching the maximum above 200 Hz, based on the data in Figure 6, which is comparable with the large strain macroscopic compression test result of  $3.59 \pm 0.11$  MPa.<sup>7</sup> High frequency deformation can induce thermal effects, which due to the PDMS low thermal conductivity result in the slight modulus reduction past 210 Hz in Figure 6(a).

Figure 7(a) shows storage modulus data obtained using the nano-DMA static force control test. The static force was varied between 2 mN and 8 mN with the set dynamic force of 50  $\mu\text{N}$ , and the frequency of either 10 Hz or 100 Hz. The difference between the loading and unloading results is due to the

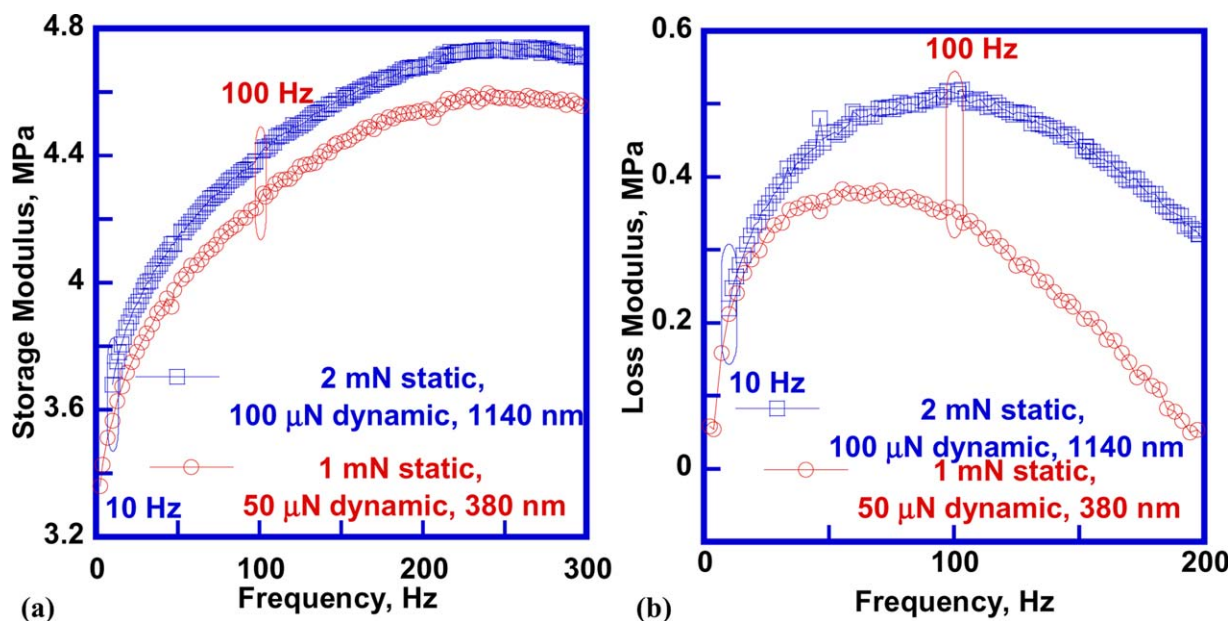


**Figure 6.** Frequency sweep nano-DMA test results: (a) storage modulus; (b) loss modulus. [Color figure can be viewed in the online issue, which is available at [wileyonlinelibrary.com](http://wileyonlinelibrary.com).]

viscoelastic PDMS properties. Similar to the quasi-static flat punch indentation, the sample appears stiffer during the unloading due to the incomplete viscoelastic recovery. In Figure 7(a), the storage modulus at 1140 nm nanoindentation depth is around 4.5 MPa, which is comparable to the data outlined in Figure 6(a). Also, the storage modulus at 380 nm nanoindentation depth with 10 Hz test frequency is around 3.5 MPa, which is similar to the data outlined in Figure 6(a). Both frequency and force control tests provide comparable results for the similar frequency and indentation depth.

Figure 7(b) shows the loss modulus obtained from the nano-DMA static force control test. The 5 : 1 PDMS loss modulus of

0.5 MPa in Figure 7(b) at the 1140 nanoindentation depth and 100 Hz test frequency is similar to the corresponding test conditions in Figure 6(b). As expected, there is not much difference between the loading and unloading tests for the loss modulus. Using eqs. (5) and (11), the maximum elastic modulus measured using the force controlled dynamic test is 3.66 MPa, which is also comparable with the large strain macroscopic compression test result of  $3.59 \pm 0.11$  MPa.<sup>7</sup>

Previous dynamic testing of PDMS, up to 100 Hz, exhibited similar results, where the storage and loss modulus increased with the indentation depth and frequency.<sup>30–32</sup> Here, the maximum elastic modulus was captured just above 210 Hz,

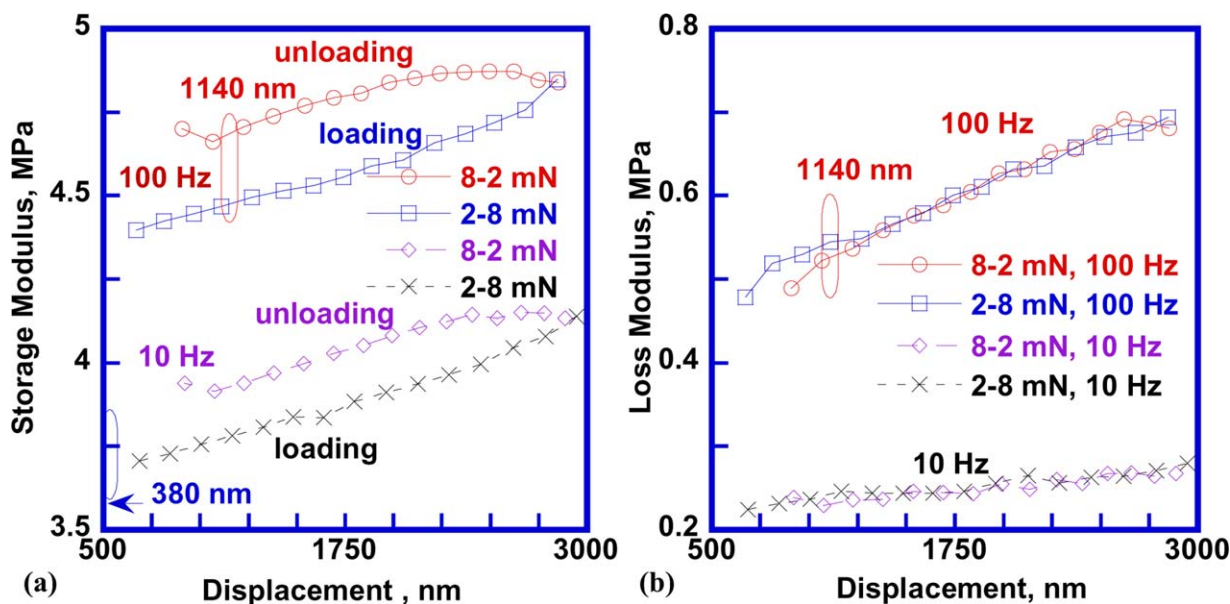


**Figure 7.** Force control nano-DMA test results: (a) storage modulus; (b) loss modulus. [Color figure can be viewed in the online issue, which is available at [wileyonlinelibrary.com](http://wileyonlinelibrary.com).]

corresponding with the large strain macroscopic compression test result. When comparing dynamic tests, one has to make sure that similar experimental conditions are used, since the measured elastic modulus strongly depends on the test frequency and indentation depth. However, the technique is sensitive enough to assess local surface stiffness variations, needed for properly assessing the adhesion behavior of live cells.

Wilder et al. study reports that the elastic modulus of the 5 : 1 PDMS sample measured in tension is 1.5 MPa, while it is above 2.65 MPa when measured using polystyrene film buckling sensors.<sup>33</sup> This sample with the 5 : 1 elastomer base to the curing agent ratio exhibited the only discrepancy between the two types of the test, compared with the rest of the samples with higher ratios, up to 25 : 1. This study shows a similar difference of elastic modulus measured using static and dynamic indentation tests.

## CONCLUSIONS

The mechanical properties of 5 : 1 PDMS were measured using quasi-static indentation with Berkovich and flat punch tips. Once accounted for the testing artifacts (pull-in for the Berkovich indenter and developing full contact for the flat punch), both tests gave comparable elastic modulus result of about 1.5 MPa. Dynamic testing with the flat punch shows strong testing frequency and depth dependence, and provides comparable results for the similar testing conditions. The elastic modulus of the 5 : 1 PDMS sample is about 3.6 MPa, which is comparable with the macroscopic compression test result. For both static and dynamic tests, PDMS unloading stiffness is higher than the loading stiffness due to the incomplete viscoelastic recovery.

## ACKNOWLEDGMENTS

The authors thank Greeshma Mohan for the samples preparation and Professor Qiao's group from the University of Science and Technology Beijing for the use of the Hysitron Triboindenter. The authors acknowledge support from the National Science Foundation (DMR1056475, CMMI1130755, CMMI0600266 and IRES1358088).

## REFERENCES

1. Joint Assessment of Commodity Chemicals No. 26. Linear Polydimethylsiloxanes (CAS No. 63148-62-9); European Center for Ecotoxicology and Toxicology of Chemicals Report: Brussels, Belgium, **1994**; p 1, ISSN 0773-6339-26.
2. Zhang, W.; Choi, D. S.; Nguyen, Y. H.; Chang, J.; Qin, L. *Sci. Rep.* **2013**, *3*, 1.
3. Brown, X. Q.; Ookawa, K.; Wong, J. Y. *Biomaterials* **2005**, *26*, 3123.
4. Eroshenko, N.; Ramachandran, R.; Yadavalli, V. K.; Rao, R. *J. Biol. Eng.* **2013**, *7*, 1.
5. Palchesko, R. N.; Ling Zhang, L.; Sun, Y.; Feinberg, A. W. *PLoS One* **2012**, *7*, e51499.
6. Carrilloa, F.; Gupta, S.; Balooch, M.; Marshall, S. J.; Marshall, G. W.; Pruitt, L.; Puttlitz, C. M. *J. Mater. Res.* **2005**, *20*, 2820.
7. Wang, Z.; Volinsky, A. A.; Gallant, N. D. *J. Appl. Polym. Sci.* **2014**, *131*, 41050.
8. Deuschle, J. K.; Buerki, G.; Deuschle, H. M.; Enders, S.; Michler, J.; Arzt, E. *Acta Mater.* **2008**, *56*, 4390.
9. Deuschle, J. K.; Enders, S.; Arzt, E. *J. Mater. Res.* **2007**, *22*, 3107.
10. Zhu, R.; Hoshi, T.; Muroga, Y.; Hagiwara, T.; Yano, S.; Sawaguch, T. *J. Appl. Polym. Sci.* **2013**, *127*, 3388.
11. Vera-Craziano, R.; Hernandez-Sanchez, F.; Cauich-Rodriguez, J. V. *J. Appl. Polym. Sci.* **1995**, *55*, 1317.
12. Carrilloa, F.; Gupta, S.; Balooch, M.; Marshall, S. J.; Marshall, G. W.; Pruitt, L.; Puttlitz, C. M. *J. Mater. Res.* **2005**, *20*, 2820.
13. Fuard, D.; Tzvetkova-Chevolleau, T.; Decossas, S. *Microelectron. Eng.* **2008**, *85*, 1289.
14. Dow Corning Corporation. Information about Dow Corning® Brand Silicone Encapsulants. Product Information. Form No. 10-898I-01, 2008. [http://www.neyco.fr/pdf/silicones\\_electronique.pdf](http://www.neyco.fr/pdf/silicones_electronique.pdf), last accessed June 16, **2014**.
15. Mullins, L. *Rubber Chem. Technol.* **1969**, *42*, 339.
16. Hansona, D. E.; Hawley, M.; Houlton, R.; Chitanvis, K.; Rae, P.; Orler, E. B.; Wroblewski, D. A. *Polymer* **2005**, *46*, 10989.
17. Godovsky, Y. K.; Papkov, V. S. In *Polymer Data Handbook*; Mark, J. E., Ed.; Oxford University Press: New York, **1999**; p 430.
18. Wang, B.; Krause, S. *Macromolecules* **1987**, *20*, 201.
19. Gorrasi, G.; Guadagno, L.; D'Aniello, C.; Naddeo, C.; Romano, G.; Vittoria, V. *Macromol. Symp.* **2003**, *203*, 285.
20. Murayama, T. *Dynamic Mechanical Analysis of Polymeric Materials*; Elsevier: New York, **1978**.
21. Odegard, G. M.; Bandorawalla, T.; Herring, H. M.; Gates, T. S. *Exp. Mech.* **2005**, *45*, 130.
22. Alisafaei, F.; Han, C.-S.; Hamid, S.; Sanei, R. *Polym. Test.* **2013**, *32*, 1220.
23. Kohn, J. C.; Ebenstein, D. M. *J. Mech. Behav. Biomed. Mater.* **2013**, *20*, 316.
24. Ebenstein, D. M. *J. Mater. Res.* **2011**, *26*, 1026.
25. Cheng, L.; Xia, X.; Yu, W.; Scriven, L. E.; Gerberich, W. W. *J. Polym. Sci. Part B: Polym. Phys.* **2000**, *38*, 10.
26. Singh, S. P.; Singh, R. P.; Smith, J. F. *Mater. Res. Soc. Symp. Proc.* **2005**, *841*, R4.6.
27. Schmid, H.; Michel, B. *Microelectron. Eng.* **2003**, *69*, 519.
28. Cao, Y.; Ma, D.; Raabe, D. *Acta Biomater.* **2009**, *5*, 240.
29. Volinsky, A. A.; Bahr, D. F.; Kriese, M. D.; Moody, N. R.; Gerberich, W. W. In *Nanoindentation Methods in Interfacial Fracture Testing*, Chapter 13: *Comprehensive Structural Integrity* (Milne, I., Ritchie, R.O., Karihaloo, B., Editors-in-Chief), Vol. 8: *Interfacial and Nanoscale Failure*; Gerberich, W. W., Yang, W., Eds.; Elsevier, **2003**; p 453.
30. Du, P.; Cheng, C.; Lu, H.; Zhang, X. *Solid-State Sensors, Actuators and Microsystems (TRANSDUCERS & EUROSENSORS XXVII)*; IEEE: Barcelona, Spain, **2013**; p 1063.
31. Du, P.; Cheng, C.; Lu, H.; Zhang, X. *J. Microelectromech. Syst.* **2013**, *22*, 44.
32. Lin, I.-K.; Ou, K.-S.; Liao, Y.-M.; Zhang, X. *J. Microelectromech. Syst.* **2009**, *18*, 1087.
33. Wilder, E. A.; Guo, S.; Lin-Gibson, S.; Fasolka, M. J.; Stafford, C. M. *Macromolecules* **2006**, *39*, 4138.